ACS Catalysis

Research Article

pubs.acs.org/acscatalysis

Ethanol Dehydration and Dehydrogenation on γ-Al_2O_3: Mechanism of Acetaldehyde Formation

Joseph F. DeWilde, Christopher J. Czopinski, and Aditya Bhan*

Department of Chemical Engineering and Materials Science University of Minnesota—Twin Cities, 421 Washington Avenue S.E., Minneapolis, Minnesota 55455, United States

Supporting Information

ABSTRACT: Steady state kinetics and measured pyridine inhibition of ethanol dehydration and dehydrogenation rates on γ-alumina above 623 K show that ethanol dehydrogenation can be described with an indirect hydrogen transfer mechanism to form acetaldehyde and ethane and that this mechanism proceeds through a shared surface intermediate with ethylene synthesis from ethanol dehydration. Ethane is produced at a rate within experimental error of acetaldehyde production, demonstrating that ethane is a coproduct of acetaldehyde synthesis from ethanol dehydrogenation. Steady state kinetic measurements indicate that acetaldehyde synthesis rates above 623 K are independent of co-fed water partial pressure up to 1.7 kPa and possess an ethanol partial pressure dependence between 0 and 1 ($P_{ethanol}$ = 1.0–16.2 kPa), consistent with ethanol dehydrogenation rates being inhibited only by ethanol monomer surface species. The surface density of catalytically active sites for ethylene and diethyl ether production were estimated from in situ pyridine titration experiments to be ~0.2 and ~1.8 sites nm^{-2}, respectively, at 623 K. Primary kinetic isotope effects for ethylene and acetaldehyde are measured only when the C–H bonds of ethanol are deuterated, verifying that C–H bond cleavage is kinetically limiting for both products. The proposed indirect hydrogen transfer model for acetaldehyde synthesis is consistent with experimentally observed reaction rate dependences and kinetic isotope effects and highlights the complementary role of hydrogen adatom removal pathways in the formation of aldehydes on Lewis acidic systems.

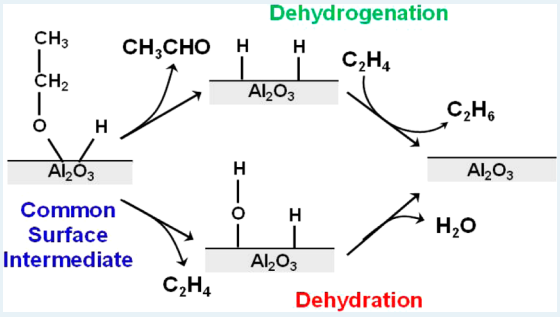

KEYWORDS: *ethanol dehydration and dehydrogenation, kinetics and mechanism, γ-alumina, acetaldehyde, ethylene, diethyl ether, site requirements*

1. INTRODUCTION

Gamma-alumina (γ-Al_2O_3), a thermally stable (up to 873 K) and high surface area (50–300 m^2 g^{-1}) Lewis acid material, is a catalyst for the industrial production of ethylene from the dehydration of ethanol.[1−7] Ethanol can dehydrate on γ-Al_2O_3 through two parallel pathways: a unimolecular pathway to form ethylene and water and a bimolecular pathway to form diethyl ether (DEE) and water.[8−21] Knözinger et al. measured the rate of cyclohexene formation from cyclohexanol dehydration and the rate of dimethyl ether formation from methanol dehydration on γ-Al_2O_3 as a function of methanol and water pressure between 433 and 468 K.[9,22] These authors observed that rates of both unimolecular and bimolecular dehydration were inhibited by water and possessed alcohol partial pressure dependences between 0 and 0.5 (7–35 kPa alcohol pressure) and described observed alcohol dehydration rates with the empirical rate equation shown below (eq 1).

$$r = r_0 \frac{\sqrt{P_A}}{\sqrt{P_A} + bP_w} \quad (1)$$

r is the synthesis rate of either olefin or ether formation, and r_0 is the synthesis rate of the products after the surface is fully saturated with alcohol (zero order in ethanol) in mol s^{-1} g^{-1}, whereas P_W and P_A are the partial pressures of water and alcohol in torr, respectively. b represents an empirically evaluated constant used to fit the measured water pressure dependence with units of torr$^{-0.5}$. Steady state kinetics of 2-propanol dehydration measured by De Morgues et al. showed that the rate of propylene synthesis at 373–433 K was independent of the partial pressure of 2-propanol (1.1–3.1 kPa) but was inversely proportional to co-fed water partial pressures (0.0–1.2 kPa), leading the authors to conclude that olefin synthesis occurs by a two-site mechanism in which water can selectively titrate one of these sites.[11] The inhibitory role of water is further supported by the combined temperature-programmed desorption and thermogravimetric analysis (TPD-TGA) measurements of 2-propanol-doused γ-Al_2O_3 samples by Roy et al., in which catalyst samples exposed to water at 373 K absorbed less 2-propanol and produced less propylene than those that were not.[16] Additionally, density functional theory (DFT) calculations performed by Jenness et al. show that water

Received: August 21, 2014
Revised: October 21, 2014
Published: November 10, 2014

   dx.doi.org/10.1021/cs501239x | ACS Catal. 2014, 4, 4425–4433

acts to inhibit ethanol dehydration on γ-Al_2O_3 by forming surface hydroxyl groups that block the C−H bond cleavage sites necessary for olefin synthesis at 500 K.[23] Shi and Davis investigated methanol and 2-butanol dehydration at a higher temperature (503 K) and found that the rates of both di-2-butyl and dimethyl ether synthesis possessed a square dependence on the alcohol pressure.[17] In previous work, we reported that synthesis rates of ethylene and DEE from ethanol dehydration on γ-Al_2O_3 at 488 K can be described with a proposed dimer-inhibited mechanism for alcohol dehydration in which ethanol dimers and ethanol−water coadsorbed complexes inhibited the rate of both dehydration pathways.[18] Our study aims to extend these prior investigations to industrially relevant temperatures (>623 K) and, in particular, to investigate the kinetic role of water and the dominant surface species at these temperatures.

Dehydration, however, is not the only pathway for alcohol conversion on γ-Al_2O_3, as alcohols can also dehydrogenate to form ketones and aldehydes.[24−26] Chokkaram et al. reported that octanone was synthesized with a selectivity between 0.3 and 0.5% from the conversion of 2-octanol on γ-Al_2O_3 at 523 K, but did not observe significant production of octanone at lower reaction temperatures.[24] Acetaldehyde synthesis was observed by Kieffer et al. upon degassing ethanol-doused samples of γ-Al_2O_3 at 473 K; the authors proposed that acetaldehyde is formed from the cleavage of a C_α−H bond of an absorbed ethoxy species.[25] DFT calculations (PW91 functional) of propane metathesis on γ-Al_2O_3-supported tungsten carbyne structures performed by Joubert et al. confirmed that the γ-Al_2O_3 support was responsible for the initial dehydrogenation of propane before continued metathesis on the organometallic complex,[26] further demonstrating the capability of γ-Al_2O_3 to activate C−H bonds for dehydrogenation. The conversion of ethanol on 0.20 g of H-ZSM-5/γ-Al_2O_3 at 623 K (total volumetric flow rate = 50 cm^3 s^{-1}) was observed to drop from 75 to 25% upon addition of 15 mol % of acetaldehyde to a liquid ethanol feed stream (0.015 cm^3 s^{-1}), demonstrating that acetaldehyde can deactivate ethanol dehydration on acidic catalytic systems.[27] Additionally, Diaz et al. noted that bands between 1300 and 1800 cm^{-1} associated with carbonyl bending modes in infrared (IR) spectra of acetaldehyde absorbed onto H-ZSM-5 at 313 K broadened and became indistinguishable when the gas phase acetaldehyde pressure was raised above 0.4 kPa. The authors attributed this broadening to the formation of large conjugated surface species produced by the condensation of acetaldehyde.[28] These large surface species are proposed to act as coke precursors responsible for catalyst deactivation.[27] The site requirements and mechanism of acetaldehyde synthesis, a critical component in understanding deactivation of ethanol conversion on acidic catalytic systems, was probed in this work with isotope labeling and in situ chemical titration studies.

In this work, the observed reactant pressure dependencies of ethylene, DEE, acetaldehyde, and ethane synthesis rates suggest that ethanol dehydrogenation operates by an indirect hydrogen transfer mechanism to form acetaldehyde and ethane and that observed rates are inhibited only by surface ethanol monomer species. The synthesis rates of ethylene, acetaldehyde, and ethane were inhibited to the same extent by pyridine, demonstrating that kinetic pathways for unimolecular dehydration and dehydrogenation of ethanol possess a common surface intermediate. The catalytic sites responsible for the bimolecular dehydration of ethanol were determined to be not equivalent to and possess a surface density an order of magnitude larger than those responsible for unimolecular dehydration using transient pyridine uptake measurements.

2. MATERIALS AND METHODS

2.1. Catalyst Preparation. γ-Al_2O_3 was used as purchased from the manufacturer (18HPa-150 Catalox, BET surface area = 141 m^2 g^{-1}, pore volume = 0.786 cm^3 g^{-1}) for each kinetic measurement. Catalyst particles between 180 and 420 μm (40−80 mesh) for steady state kinetic measurements at 623 K and between 180 and 250 μm (60−80 mesh) for all other measurements were collected after sieving compressed γ-Al_2O_3 powder. The catalyst particles were then individually counted and weighed to obtain the small catalyst amounts used in the kinetic measurements (0.3−1.0 mg). The catalyst bed was then combined with acid-washed quartz sand and treated in air as previously described.[18] Prior to each experiment, the catalyst was exposed to 2.2 kPa of deionized water in He (total flow rate = 1.7 cm^3 s^{-1}) to induce the previously observed partial deactivation of the catalytic surface by water adsorption.[18]

2.2. Steady State Kinetic Measurements of Ethanol Conversion over γ-Al_2O_3. Steady state kinetic measurements of ethanol conversion on γ-Al_2O_3 were performed using the reactor system described previously.[18] Ethanol conversion kinetic measurements were carried out at 623, 648, and 673 K using a He carrier gas (grade 4.7, Minneapolis Oxygen Co.) with a flow rate of 9.9 cm^3 s^{-1} at ambient pressure. An internal standard mixture of 25.0% CH_4 with a balance of Ar (Minneapolis Oxygen Co.) was also fed at 0.017 cm^3 s^{-1} at NTP conditions for gas chromatography analysis. Differential conversion of ethanol (<10%) was maintained by using 0.3−1.0 mg of catalyst at temperatures between 623 and 673 K.

The partial pressure of ethanol (99.5% Decon Laboratories, Inc.) in the feed was varied between 1.0 and 16.2 kPa for kinetic investigations and was maintained by controlling the liquid flow rate into the system. Pyridine (99+%, Sigma-Aldrich) was similarly fed to maintain a feed partial pressure between 0.0 and 0.7 kPa for steady state pyridine inhibition measurements at 673 K. Kinetic isotope studies using C_2H_5OD and C_2D_5OD (99.5 at. % D, Sigma-Aldrich) reagents were done at 3.1 kPa partial pressure of the alcohol reactant. For all experiments, a deionized water co-feed was maintained between 0.5 and 1.7 kPa. All steady state kinetic measurements were compared and normalized to the initial experimental condition that was repeated after every change in the feed composition and was used as a reference to account for any deactivation of the catalyst during the reaction (Figure S1).

The composition of the reactor effluent was determined using both a gas chromatograph (GC) and an online mass spectrometer (MS) as described previously.[18] Reported errors were determined by evaluating the 95% confidence interval of repeated titrations or successive GC measurements at the same experimental set points.

2.3. In Situ Pyridine Titration of Catalytic Sites Responsible for Ethanol Dehydration. The transient profile of ethylene and DEE production from the dehydration of 3.0 kPa of ethanol with a deionized water co-feed of 1.3 kPa over 0.0015−0.020 g of γ-Al_2O_3 at 623 K was measured using online mass spectrometry after the introduction of a steady 0.05−0.10 kPa stream of pyridine. The measured transient effluent composition profile was used with the evaluated kinetics for ethylene and DEE formation to determine the uptake of pyridine necessary to completely deactivate both

dx.doi.org/10.1021/cs501239x | ACS Catal. 2014, 4, 4425−4433

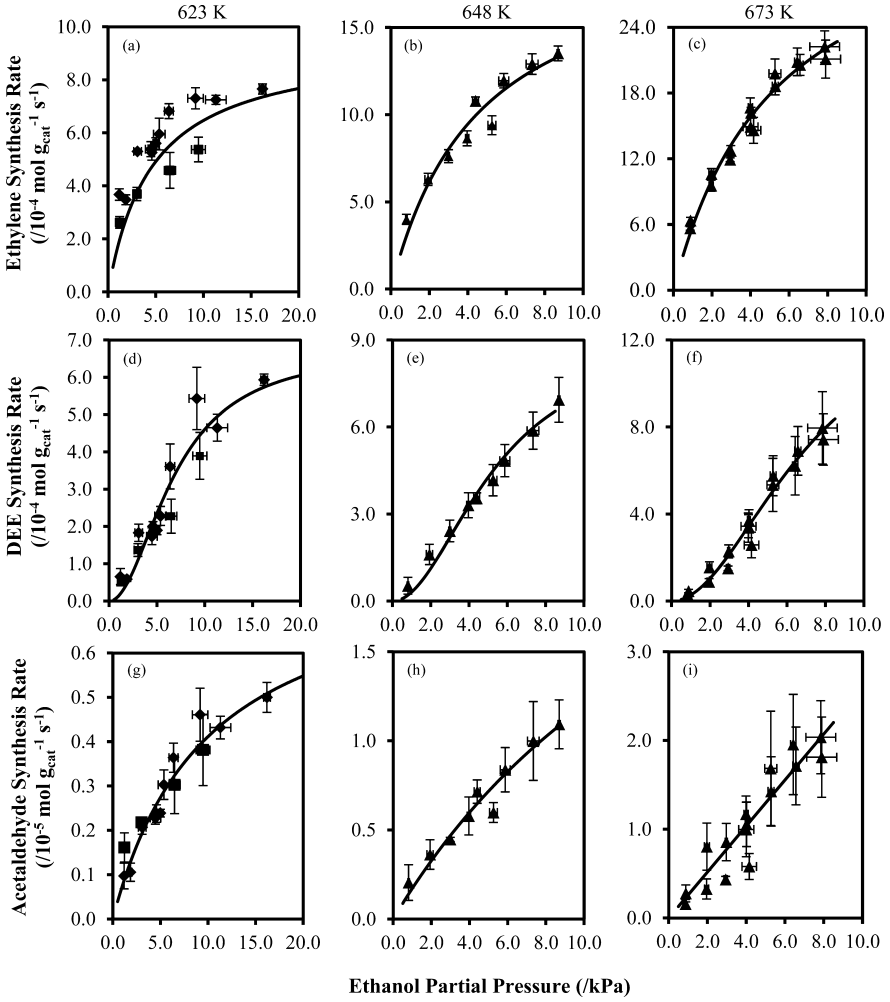

Figure 1. (a–c) Ethylene, (d–f) DEE, and (g–i) acetaldehyde synthesis rates as a function of ethanol pressure at (a, d, g) 623 K, (b, e, h) 648 K, and (c, f, i) 673 K and with 1.5 kPa (◆), 0.6 kPa (■), and 0.4 kPa (▲) of co-fed water partial pressure over (a, d, g) 1.0 mg, (b, e, h) 0.5 mg, and (c, f, i) 0.3 mg of γ-Al_2O_3 (total volumetric flow rate = 9.9 cm^3 s^{-1}). The solid lines represent model fits to eqs (a–c) 2, (d–f) 3, and (g–i) 4.

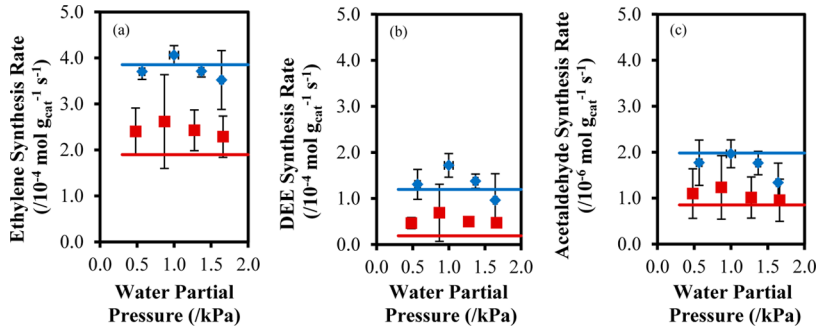

Figure 2. (a) Ethylene, (b) DEE, and (c) acetaldehyde synthesis rates from the conversion of 3.2 kPa (blue diamonds) and 1.2 kPa (red squares) of ethanol as a function of co-fed water partial pressure over 1.0 mg of γ-Al_2O_3 (total volumetric flow rate = 9.9 cm^3 s^{-1}) at 623 K. The solid lines represent model fits to eqs (a) 2, (b) 3, and (c) 4.

dehydration pathways and thereby estimate the surface density of catalytic sites responsible for the formation of the two products.

2.4. Evaluation of Reported Kinetic Parameters. The kinetic parameters presented in section 3.1 were estimated by optimizing the model fits to the presented data using Bayesian statistical optimization techniques and the Athena Visual Studio (v14.2, W. E. Stewart and M. Caracotsios) statistical software package. The reported uncertainties represent the 95% marginal highest posterior density intervals. Experimental replicates were provided from repeated independent measurements of ethanol dehydration and dehydrogenation rates on fresh catalyst samples.

3. RESULTS AND DISCUSSION

3.1. Kinetics of Ethylene, DEE, and Acetaldehyde Synthesis above 623 K. The synthesis rates of ethylene and DEE from ethanol dehydration on γ-Al_2O_3 between 623 and

dx.doi.org/10.1021/cs501239x | ACS Catal. 2014, 4, 4425–4433

Table 1. Estimated Values for the Kinetic Parameters of Ethylene, DEE, and Acetaldehyde Formation over γ-Al_2O_3 at 623, 648, and 673 K Using the Models Presented in Equations 2−4 and the Data from Figures 1 and 2

	ethylene (eq 2)		DEE (eq 3)		acetaldehyde (eq 4)	
parameter	$k_{C_2H_4}$ ($/10^{-4}$ $mol_{C_2H_4}$ s^{-1} g^{-1})	K_{A1} (kPa^{-1})	k_{DEE} ($/10^{-4}$ mol_{DEE} s^{-1} g^{-1})	$K_{A1}K_{A2}$ (kPa^{-2})	k_{CH_3CHO} ($/10^{-5}$ mol_{CH_3CHO} s^{-1} g^{-1})	K_{A1} (kPa^{-1})
value (623 K)	9.4 ± 3.3	0.22 ± 0.17	6.8 ± 1.2	0.021 ± 0.009	0.82 ± 0.19	0.10 ± 0.04
value (648 K)	20.4 ± 6.5	0.22 ± 0.15	9.1 ± 1.8	0.035 ± 0.015	3.5 ± 3.6	0.05 ± 0.07
value (673 K)	37.0 ± 5.9	0.19 ± 0.06	14.2 ± 3.6	0.020 ± 0.009	$k_{CH_3CHO}K_{A1}$ = 0.26	

673 K possess ethanol partial pressure dependences with an order between 0.2 and 0.6 for ethylene synthesis and between 0.6 and 1.5 for DEE synthesis (ethanol pressures between 1.0 and 16.2 kPa; Figure 1). Additionally, both ethylene and DEE synthesis rates are independent of co-fed water partial pressure at water pressures <1.7 kPa at these temperatures (Figure 2), consistent with Langmuir−Hinshelwood mechanisms for both unimolecular and bimolecular ethanol dehydration pathways in which only the reactive precursor before the rate-limiting step (ethanol monomers for ethylene synthesis and ethanol dimers for DEE synthesis) inhibits observed rates.

Previously we noted that both the unimolecular and bimolecular dehydration of ethanol on γ-Al_2O_3 at 488 K could be described by surface mechanisms in which the reactions were inhibited by dimer species composed of ethanol and water surface species.[18] The observed kinetic dependences on ethanol and water pressure suggest that dimeric surface species are not sufficiently stable at temperatures above 623 K to have a measurable effect on the rate of dehydration.

In addition to ethylene and DEE from the dehydration of ethanol at temperatures above 623 K, acetaldehyde is observed as a product of ethanol dehydrogenation on γ-Al_2O_3 at a rate that is >2 orders of magnitude slower than that of the unimolecular dehydration of ethanol. Acetaldehyde synthesis occurs at a rate that is independent of co-fed water partial pressure and possesses an ethanol partial pressure dependence of orders between 0.4 and 1.0 (Figures 1 and 2), indicating that, much like ethylene synthesis, acetaldehyde synthesis can be modeled considering a surface mechanism inhibited by only a reactive intermediate surface species.

The kinetic models for ethylene, DEE, and acetaldehyde synthesis presented in eqs 2, 3, and 4, respectively, can be derived by assuming that (1) the rate-limiting step is the decomposition of a surface species to form each product,[18] (2) the only significant surface species is the reactive surface intermediate (an ethanol monomer species for ethylene and acetaldehyde synthesis and a bimolecular coadsorbed ethanol dimer species for DEE synthesis), and (3) these reactive surface intermediates are in quasi-equilibrium with gaseous ethanol.

$$r_{C_2H_4} = \frac{k_{C_2H_4}K_{A1}P_{EtOH}}{1 + K_{A1}P_{EtOH}} \quad (2)$$

$$r_{DEE} = \frac{k_{DEE}K_{A1}K_{A2}P_{EtOH}^2}{1 + K_{A1}K_{A2}P_{EtOH}^2} \quad (3)$$

$$r_{CH_3CHO} = \frac{k_{CH_3CHO}K_{A1}P_{EtOH}}{1 + K_{A1}P_{EtOH}} \quad (4)$$

$r_{C_2H_4}$, r_{DEE}, and r_{CH_3CHO} are the synthesis rates of ethylene, DEE, and acetaldehyde, respectively. $k_{C_2H_4}$, k_{DEE}, and k_{CH_3CHO} represent the intrinsic rate constants for each reaction. K_{A1} represents the equilibrium constant of adsorption to form a reactive ethanol monomer surface species from gas phase ethanol, hypothesized to be either a surface ethoxy species[18] or a strongly adsorbed ethanol molecule,[29] whereas K_{A2} is the equilibrium constant for a second gas phase molecule to adsorb onto the first ethanol surface species to form a reactive coadsorbed ethanol dimer surface species for DEE synthesis.[18] Finally, P_{EtOH} is the gas phase ethanol pressure. The values of each of the kinetic parameters at 623, 648, and 673 K were estimated using the data presented in Figures 1 and 2 and are reported in Table 1. The solid lines in Figures 1 and 2 show the model fit to the experimental data. Parity, lag, and normal probability plots for the models at each temperature are presented in Figures S2, S3, and S4, respectively.

An alternative rate expression to the one presented in eq 3 for DEE synthesis that includes the surface coverage of ethanol monomer species can also be proposed. This rate expression, however, does not statistically reduce the residual error or improve the model's ability to describe the measured kinetics over the one presented in eq 3, indicating that the ethanol pressure range in which ethanol monomer species dominate the catalyst surface is relatively small compared to our ability to accurately measure the rate. The mathematically simpler model presented in eq 3 was chosen as the rate expression to minimize the number of kinetic parameters needed to describe the measured synthesis rates.

The high relative uncertainties of the reported equilibrium constants of adsorption are a result of the relatively few measured data points in which the coverage of reactive surface species is kinetically relevant. Over the majority of the tested ethanol pressures, the surface coverage of adsorbates was sparse, and empty sites were the predominantly prevalent surface species. Furthermore, the coverage of reactive surface species for acetaldehyde synthesis was not observed to be kinetically relevant at any of the tested ethanol pressures at 673 K. Reactive precursors became kinetically relevant only at ethanol pressures above 5.0 kPa at 623 K.

The large uncertainty in acetaldehyde formation rates (Figures 1 and 2) and in the associated kinetic parameters (Table 1) is a result of the small amount of acetaldehyde generated in this process (<100 ppm of the effluent stream), making accurate quantitation difficult. The small concentrations, however, may still be sufficient to induce deactivation of the catalyst during reaction (Figure S1).

3.2. Kinetic Isotope Effects (KIE) for the Conversion of Ethanol at 623 K. KIE at 623 K for ethylene, DEE, and acetaldehyde from the conversion of C_2H_5OD and C_2D_5OD on γ-Al_2O_3 are reported in Table 2. A primary kinetic isotope effect (k_H/k_D = 1.9) is observed for ethylene synthesis when C_2D_5OD is fed but not when C_2H_5OD is used as a reactant, verifying that either C−H bond cleavage or the removal of water from the γ-Al_2O_3 surface is rate limiting for unimolecular ethanol

dx.doi.org/10.1021/cs501239x | ACS Catal. 2014, 4, 4425−4433

Table 2. Measured Kinetic Isotope Effects for Ethylene and Diethyl Ether Formation at 623 K for the Dehydration of 3.1 kPa of C_2H_5OD and C_2D_5OD over 1.0 mg of γ-Al_2O_3 and 1.5 kPa of Water Co-feed

	reactant	
product	C_2H_5OD	C_2D_5OD
ethylene KIE (r_H/r_D)	0.99 ± 0.01	1.9 ± 0.1
diethyl ether KIE (r_H/r_D)	0.98 ± 0.03	1.0 ± 0.2
acetaldehyde KIE (r_H/r_D)	1.09 ± 0.02	1.6 ± 0.2

dehydration. Conversely, no kinetic isotope effect was observed for either labeled reactant for DEE synthesis, demonstrating that either C−O bond cleavage or Al−O bond cleavage of a surface intermediate is the rate-limiting step for the bimolecular dehydration of ethanol. The measured KIE at 623 K and our inferences are consistent with our previous investigation at 488 K[18] and with observed KIE of the dehydration of deuterium-labeled methanol, iso-butanol, *tert*-butanol, and sec-butanol reported by Knözinger et al.[30,31] DFT calculations (PW91 functional with generalized gradient approximation) of ethanol dehydration on γ-Al_2O_3 performed by Christiansen et al. also note that C_β−H bond cleavage is limiting in ethylene synthesis (activation energy = 37 kcal mol^{-1}) and that an S_N2 reaction step involving the cleavage of the C−O bond of ethanol is rate limiting in DEE synthesis (activation energy = 35 kcal mol^{-1}).[29]

Much like ethylene synthesis, a primary kinetic isotope effect was observed for acetaldehyde synthesis (k_H/k_D = 1.6) only for the fully deuterated reactant and not for C_2H_5OD, indicating that acetaldehyde synthesis is similarly limited by the cleavage of either an O−H bond of a surface-bound hydrogen adatom or a C−H bond. We postulate that ethanol dehydrogenation on γ-Al_2O_3 is limited by the cleavage of a C_α−H bond of an adsorbed ethoxy species rather than by the cleavage of the C_β−H bond to from a surface enolate that subsequently undergoes rapid hydride transfer to form acetaldehyde. Measured KIEs of $(CH_3)_2CDOH$ dehydrogenation into acetone over Ni/γ-Al_2O_3 at 333 K observed by Shimizu et al.[32] (k_H/k_D = 2.0) and over Cr_2O_3 at 623 K observed by Nondek and Sedláček (k_H/k_D = 1.9)[33] mirror our proposed rate-limiting step for alcohol dehydrogenation on γ-Al_2O_3. Additionally, prominent infrared bands associated with surface ethoxy species (1000−1100 and 2800−3000 cm^{-1}) and the corresponding production of acetaldehyde were observed in in situ IR spectroscopic measurements of CeO_2 in the presence of flowing ethanol at 523 K by Li et al., leading the authors to also conclude that acetaldehyde synthesis is limited by the C_α−H bond cleavage of an absorbed ethoxide species.[34]

3.3. Ethane Synthesis and Acetaldehyde Formation Mechanism. Ethane is also seen as a product of ethanol conversion above 623 K and is synthesized at rates that are in a 1:1 ratio with acetaldehyde production within experimental error (Figure 3), signifying that ethane is a coproduct of acetaldehyde synthesis. Ethane was also observed by Phung et al. as a product of ethanol conversion on γ-Al_2O_3 at 623 K with a similar selectivity (~1.0%).[35] Furthermore, the synthesis rates of both ethane and acetaldehyde at 673 K are independent of co-fed ethylene pressure up to 1.5 kPa (Figure 4), indicating acetaldehyde is not formed by a direct hydrogen transfer pathway in which ethanol transfers hydrogen to ethylene in the rate-limiting step.

Two mechanisms for acetaldehyde synthesis consistent with the measured KIE for acetaldehyde formation, the 1:1

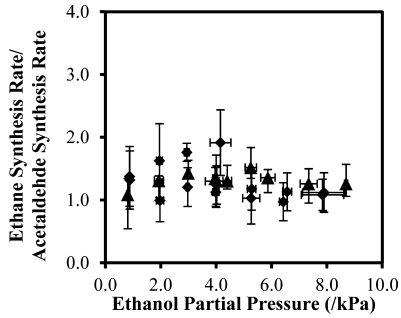

Figure 3. Ratio of the ethane and acetaldehyde synthesis rates formed in ethanol dehydrogenation reactions over 0.3 mg of γ-Al_2O_3 (total volumetric flow rate = 9.9 cm^3 s^{-1}) at 648 K (▲) and 673 K (◆) with a water co-feed of 0.4 kPa as a function of ethanol pressure.

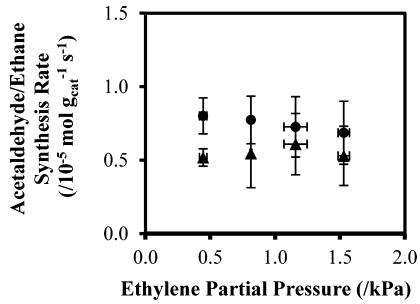

Figure 4. Acetaldehyde (▲) and ethane (●) synthesis rates from the conversion of 3.0 kPa of ethanol over 0.3 mg of γ-Al_2O_3 at 673 K with a water co-feed of 0.4 kPa as a function of co-fed ethylene partial pressure.

stoichiometric production of ethane and the independence of acetaldehyde synthesis rates on ethylene partial pressure, are presented in Scheme 1. Scheme 1a shows the dehydrogenation of ethanol limited by C_α−H bond cleavage of a surface ethoxy species to form acetaldehyde and two surface-bound hydrogen adatoms, which subsequently desorb to form gas phase hydrogen. Ethylene would then undergo hydrogenation with the molecular hydrogen formed in a microscopic reverse of the dehydrogenation of alkanes investigated in DFT calculations by Wischert et al.[36,37] and as demonstrated in the reactive TPD experiments of ethylene-exposed γ-Al_2O_3 in the presence of hydrogen gas at room temperature by Amenomiya et al.[38] Scheme 1b displays an indirect hydrogen transfer mechanism, which is also limited by the cleavage of the C_α−H of a surface ethoxy species. Ethylene is instead hydrogenated by hydrogen adatoms to regenerate the catalytic surface. The synthesis of ethane was not observed to be catalyzed by γ-Al_2O_3 upon feeding 0.8 kPa of ethylene and 4.2 kPa of hydrogen in independent kinetic studies (hydrogen pressures used are 4000 times higher than the outlet pressure of acetaldehyde at 673 K), over 0.3 mg of catalyst at 673 K, favoring the indirect hydrogen transfer mechanism depicted in Scheme 1b.

3.4. Site Density Measurements for Ethanol Dehydration on γ-Al_2O_3. Previously, we employed in situ titration with pyridine to estimate the surface density of catalytic sites responsible for DEE formation at 488 K and under differential catalytic conditions (~0.1 site nm^{-2}).[18] At temperatures >623 K, the small catalyst loading required to achieve differential ethanol conversions (~1.0 mg) is insufficient for accurate titration in the method previously described;[18] therefore, in situ titrations with pyridine must be performed at higher

dx.doi.org/10.1021/cs501239x | ACS Catal. 2014, 4, 4425−4433

Scheme 1. Acetaldehyde Synthesis Mechanisms from Ethanol Dehydrogenation over γ-Al_2O_3 through (a) a Direct Dehydrogenation Pathway Forming Gaseous Hydrogen and (b) an Indirect Hydrogen Transfer Pathway Forming Ethane

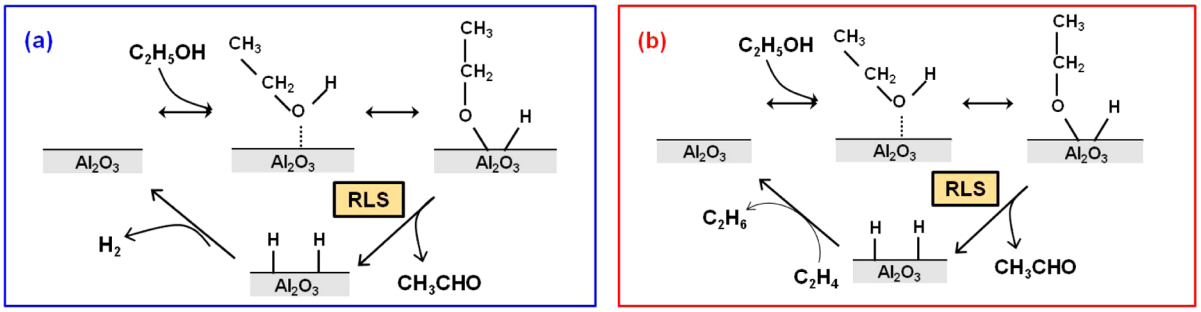

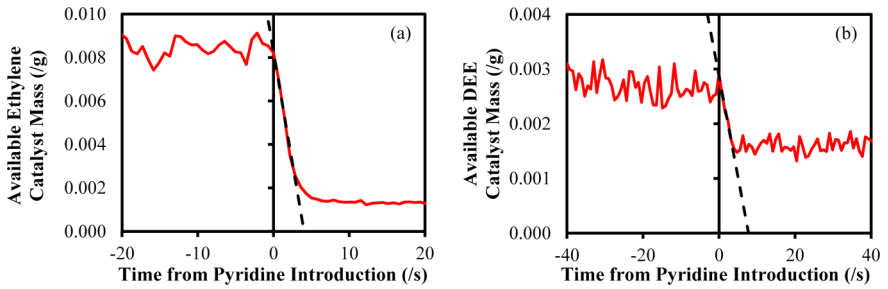

Figure 5. Available catalyst mass for the synthesis of (a) ethylene and (b) DEE from the dehydration of 3.0 kPa of ethanol on (a) 0.010 g and (b) 0.0022 g of γ-Al_2O_3 at 623 K with a 1.3 kPa water co-feed as a function of time after introduction to 0.10 kPa of pyridine in the gas stream (total gas flow rate = 9.9 $cm^3\ s^{-1}$). The available catalyst mass was estimated from eqs (a) 2 and (b) 3 and the parameters in Table 1. The dashed line shows the linear extrapolation used to estimate the total catalytic site density for ethylene synthesis.

conversions (up to 70%). The transient effluent composition of the reactor can be used to determine the active catalyst mass in the reactor using eqs 2 and 3 by assuming a plug flow reactor model. Assuming that far from equilibrium every molecule of pyridine that enters the bed of the reactor titrates a catalytically active site and that each active site contributes equally to the catalytic activity, the transient profile of the active catalyst mass should decrease linearly upon introduction to a constant feed of pyridine until an equilibrium coverage of pyridine is achieved (Figure 5). The total uptake of pyridine necessary to completely shut down the production of either ethylene or DEE was estimated by extrapolating this linear inhibition regime. The estimated pyridine surface density needed to completely deactivate the synthesis of ethylene and DEE and, thus, the density of catalytic sites responsible for these reactions at different pyridine pressures and catalyst loadings are presented in Table 3.

Table 3. Catalytic Site Density for Ethylene and DEE Synthesis from Ethanol Dehydration on γ-Al_2O_3 at 623 K Estimated from Extrapolation of in Situ Titrations Using Pyridine Performed at Different Catalyst Loadings and Pyridine Partial Pressures[a]

	catalytic site density ($/10^{-5}$ mol g^{-1})			
	ethylene synthesis		DEE synthesis	
pyridine pressure (/kPa)	0.020 g of catalyst	0.010 g of catalyst	0.0022 g of catalyst	0.0015 g of catalyst
0.10	4.2 ± 0.5	5.0 ± 0.9	51 ± 7	54 ± 33
0.05	3.8 ± 0.8	4.1 ± 0.0	32 ± 8	31 ± 4

[a]The reported errors are 95% confidence intervals determined using independent titrations.

The estimated density of catalytic sites responsible for the formation of ethylene was consistent within error across multiple catalyst loadings and pyridine pressure with an average site density of $(4.1 \pm 0.3) \times 10^{-5}$ mol g^{-1} (~0.18 site nm^{-2}). The estimated density of sites responsible for DEE synthesis appears to be a function of fed pyridine pressure, signifying that the estimated density has some systematic inaccuracies likely caused by (i) uncertainties in the kinetic model for DEE synthesis causing the catalytic site density to be underestimated at lower pyridine pressures or (ii) nonuniformities in active site reactivities leading to an incomplete titration of less reactive surface sites at lower pyridine pressures. The average density of sites responsible for DEE production, however, is an order of magnitude greater than that of sites responsible for ethylene production, $(4.2 \pm 0.9) \times 10^{-4}$ mol g^{-1} or ~1.8 sites nm^{-2}. The large difference in site densities is consistent with steady state kinetic measurements in the presence of pyridine in previous investigations,[18] which indicate that the sites that catalyze ethylene and DEE synthesis are not equivalent. These results are insufficient, however, to determine whether the sites responsible for ethylene synthesis are a subset of those responsible for DEE synthesis as pyridine is an unspecific titrant for the two dehydration pathways. The values presented in Table 3 represent an upper bound of catalytic site density as pyridine could also be adsorbing onto noncatalytic surface sites in addition to the active sites. This technique, however, presents a method to estimate the density of catalytically active sites under reaction conditions and, thus, is useful as a probe for assessing catalytic site requirements and can provide a more realistic estimate of surface density than ex situ measurements. The structure of the active sites is not elucidated using this technique, and other analytical techniques will need to be applied to provide a complete picture of the catalytic system.

dx.doi.org/10.1021/cs501239x | ACS Catal. 2014, 4, 4425−4433

The density of sites responsible for DEE synthesis at 488 K was estimated to be ~0.1 site nm^{-2} in previous investigations using the same in situ titration technique, an order of magnitude less than the density estimated at 623 K.[18] This increase in active site density with temperature is reflected in DFT calculations (PW91 functional) by Digne et al., in which the stable surface coverage of hydroxyl groups formed from dissociated water decreased from 8.8 to 0 OH nm^{-2} and from 11.8 to 8.9 OH nm^{-2} on the (100) and (110) facets of γ-Al_2O_3, respectively, upon increase in the temperature from 488 to 623 K.[14,39] We postulate that the additional surface Al atoms on the dehydrated γ-Al_2O_3 surface at 623 K act as catalytic sites for DEE synthesis and explain the estimated increase in site density. Weak Lewis acid sites that become catalytically active only at elevated temperatures present another potential source for the additional catalytic sites measured at 623 K.

3.5. Site Requirements for Acetaldehyde Synthesis on γ-Al_2O_3. Pyridine was found to inhibit the syntheses of ethylene and DEE to different extents at 488 K, indicating that the catalytic sites of unimolecular and bimolecular ethanol dehydration are both acidic and nonequivalent.[18] This result is consistent with steady state kinetic measurements of ethanol conversion in the presence of pyridine on γ-Al_2O_3 at 673 K (Figure 6). The appearance of multiple infrared adsorption bands around 1450 cm^{-1} upon the exposure of pyridine to γ-Al_2O_3 led Parry[40] and Morterra and Magnacca[41] to conclude that acid sites with a distribution of strengths are present on the catalyst surface. A distribution of water adsorption and dissociation energies and, thus, acid site strengths on the γ-Al_2O_3 surface was also observed in DFT calculations (PW 91 functional) by Digne et al.[14] and Wischert et al.,[37] supporting the conclusion that different sets of catalytic sites exist on the surface of γ-Al_2O_3. Additionally, simulated and experimental $^1\{H\}^{27}Al$ cross-polarization nuclear magnetic resonance (NMR) measurements performed by Wischert et al. found that both chemical shift (10−70 ppm) and quadropolar coupling constants (5−38 MHz) are dependent on surface aluminum atom coordination and hydration state and that a distribution of these NMR parameters and, thus, potential catalytic sites can be observed on the γ-Al_2O_3 samples treated at 573 and 773 K.[42]

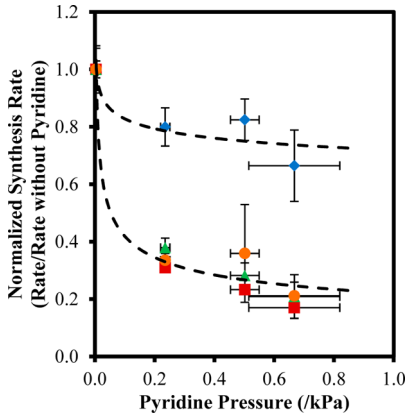

Figure 6. Ethylene (red squares), DEE (blue diamonds), acetaldehyde (green triangles), and ethane (orange circles) synthesis rates from the conversion of 3.3 kPa of ethanol over 0.3 mg of γ-Al_2O_3 at 673 K with a 0.5 kPa co-feed of water normalized to the synthesis rates observed in the absence of pyridine plotted as a function of pyridine partial pressure. The dashed lines serve as a guide for the eye.

Acetaldehyde, ethylene, and ethane production are inhibited to the same extent by pyridine (Figure 6), leading us to infer that acetaldehyde and ethane formation require acidic surface sites and that the synthesis mechanisms of both acetaldehyde and ethylene proceed through a common surface intermediate. Surface ethoxy species present one possible surface intermediate that can act as a precursor to both ethylene and acetaldehyde synthesis (Scheme 2). The relative synthesis rates of ethylene and acetaldehyde are therefore determined by the rates of C_β−H and C_α−H bond scission, respectively, of this common surface ethoxy intermediate, consistent with the measured KIEs for ethanol conversion at 623 K (Table 2).

Scheme 2. Proposed Mechanism for the Combined Synthesis Pathways of Ethylene and Acetaldehyde from a Common Ethoxy Surface Intermediate on γ-Al_2O_3

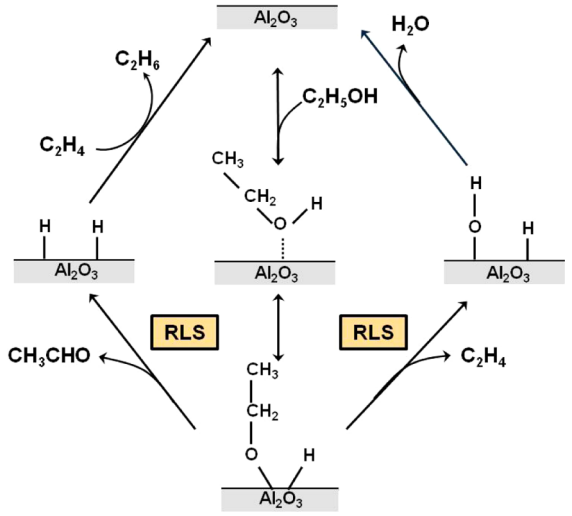

Christiansen et al. found using periodic DFT calculations (PW91 functional) that ethylene synthesis proceeds by the simultaneous cleavage of the C_β−H bond and C−O bond of an adsorbed ethanol molecule on the γ-Al_2O_3 surface rather than through a surface ethoxy intermediate.[29] This mechanism for ethylene synthesis is also consistent with the data presented in Figure 6 and with the conclusion that ethylene and acetaldehyde synthesis share a common reactive intermediate, in this case an absorbed ethanol molecule instead of an ethoxy intermediate. In this kinetically equivalent alternative mechanism, (1) acetaldehyde synthesis proceeds through the cleavage of the C_α−H bond of a surface ethoxy species that was formed from an absorbed ethanol molecule (as seen in Schemes 1 and 2), (2) ethylene synthesis would be kinetically limited by the simultaneous cleavage of the C_β−H bond and the C−O bond of an adsorbed ethanol molecule, and (3) pyridine would inhibit the adsorption of ethanol onto this shared catalytic site, thereby inhibiting acetaldehyde, ethane, and ethylene synthesis equivalently.

The inhibitory effects by pyridine, measured KIE, and steady state kinetics elucidate the role acidic surface sites, surface-bound ethoxy intermediates, and the indirect transfer of hydrogen adatoms to ethylene play in ethanol dehydrogenation on γ-Al_2O_3 above 623 K. These conclusions offer crucial considerations for catalytic design of Lewis acidic systems to

dx.doi.org/10.1021/cs501239x | ACS Catal. 2014, 4, 4425−4433

avoid the synthesis of aldehydes that may contribute to catalyst deactivation.[27,28]

4. CONCLUSIONS

Steady state kinetic measurements of ethanol dehydration and dehydrogenation reactions on γ-Al_2O_3 above 623 K reveal (1) the rates of formation of ethylene, DEE, and acetaldehyde are independent of co-fed water partial pressure; (2) the synthesis rates of ethylene and acetaldehyde possess an order between 0 and 1 for ethanol partial pressure; and (3) the synthesis rate of DEE possesses an ethanol order between 0 and 2. These observations imply that rates of ethylene, DEE, and acetaldehyde formation can be described by a surface-catalyzed mechanism inhibited only by reactive precursors (ethanol monomer species for ethylene and acetaldehyde syntheses and coadsorbed ethanol dimer species for DEE synthesis) above 623 K. Primary kinetic isotope effects were observed for ethylene and acetaldehyde synthesis at 623 K when C_2D_5OD was used as a reactant but not when C_2H_5OD was used, verifying that the cleavage of a C−H bond is rate limiting for the synthesis of these products, likely the C_β−H bond for ethylene formation and the C_α−H bond for acetaldehyde formation. A kinetic isotope effect was not measured for DEE synthesis at 623 K using either reactant, signifying that the C−O bond of ethanol is cleaved in the rate-limiting step of DEE synthesis. Ethane is produced with the same selectivity as acetaldehyde, indicating that ethane is a coproduct of ethanol dehydrogenation. The surface densities of the catalytic sites responsible for ethylene and DEE synthesis on γ-Al_2O_3 at 623 K were estimated to be 0.18 and 1.8 sites nm^{-2}, respectively, using in situ titration with pyridine. Ethylene, acetaldehyde, and ethane syntheses are inhibited to the same extent by pyridine, demonstrating that ethylene and acetaldehyde formation occur through a shared reactive intermediate. An indirect hydrogen transfer mechanism for acetaldehyde synthesis that proceeds through a shared ethoxy intermediate with ethylene synthesis and in which hydrogen adatoms are transferred to ethylene after the rate-limiting step to regenerate the catalyst surface is consistent with the presented conclusions.

■ ASSOCIATED CONTENT

Supporting Information

The following file is available free of charge on the ACS Publications website at DOI: 10.1021/cs501239x.

Analysis of deactivation and residual error in the kinetic models for ethanol conversion (PDF)

■ AUTHOR INFORMATION

Corresponding Author

*(A.B.) E-mail: abhan@umn.edu. Phone: (612) 626-3981. Fax: 612-626-7246.

Notes

The authors declare no competing financial interest.

■ ACKNOWLEDGMENTS

Financial support from The Dow Chemical Company is gratefully acknowledged. We also acknowledge Marcello Herrera and Minje Kang for their support in creating catalyst weight and gas chromatograph calibrations for this reactor system and for testing the hydrogenation of ethylene on this catalyst.

■ REFERENCES

(1) Lippens, B. C.; De Boer, J. H. *Acta Crystallogr.* **1964**, *17*, 1312−1321.
(2) Slade, R. C. T.; Southern, J. C.; Thompson, I. M. *J. Mater. Chem.* **1991**, *1*, 563−568.
(3) Cesteros, Y.; Salagre, P.; Medina, F.; Sueiras, J. E. *Chem. Mater.* **1999**, *11*, 123−129.
(4) Kogel, J. E., Trivedi, N. C., Barker, J. M., Krukowski, S. T., Eds. *Industrial Minerals & Rocks*, 7th ed.; Society for Mining, Metallurgy, and Exploration: Englewood, CO, USA, 2006; 1568 pp.
(5) Chorkendorff, I.; Niemantsverdriet, J. W. *Catalyst Supports: Alumina*; Wiley-VCH: Weinheim, Germany, 2007; Vol. 2, pp 193−195.
(6) Kwak, J. H.; Peden, C. H. F.; Szanyi, J. *J. Phys. Chem. C* **2011**, *115*, 12575−12579.
(7) Kostestkyy, P.; Yu, J.; Gorte, R. J.; Mpourmpakis, G. *Catal. Sci. Technol.* **2014**, *4*, 3861−3869.
(8) Knözinger, H. *Angew. Chem., Int. Ed.* **1968**, *7*, 791−805.
(9) Knözinger, H.; Bühl, H.; Ress, E. *J. Catal.* **1968**, *12*, 121−128.
(10) Knözinger, H.; Bühl, H.; Kochloefl, K. *J. Catal.* **1972**, *24*, 57−68.
(11) de Mourgues, L.; Peyron, F.; Trambouze, Y.; Prettre, M. *J. Catal.* **1967**, *7*, 117−125.
(12) DeCanio, E. C.; Nero, V. P.; Bruno, J. W. *J. Catal.* **1992**, *135*, 444−457.
(13) Kibby, C. L.; Lande, S. S.; Hall, W. K. *J. Am. Chem. Soc.* **1972**, *94*, 214−220.
(14) Digne, M.; Sautet, P.; Raybaud, P.; Euzen, P.; Toulhoat, H. *J. Catal.* **2004**, *226*, 54−68.
(15) Morávek, V.; Kraus, M. *J. Catal.* **1984**, *87*, 452−460.
(16) Roy, S.; Mpourmpakis, G.; Hong, D.; Vlachos, D. G.; Bhan, A.; Gorte, R. J. *ACS Catal.* **2012**, *2*, 1846−1853.
(17) Shi, B. C.; Davis, B. H. *J. Catal.* **1995**, *157*, 359−367.
(18) DeWilde, J. F.; Chiang, H.; Hickman, D. A.; Ho, C. R.; Bhan, A. *ACS Catal.* **2013**, *3*, 798−807.
(19) Kwak, J.; Mei, D.; Peden, C. F.; Rousseau, R.; Szanyi, J. *Catal. Lett.* **2011**, *141*, 649−655.
(20) Spivey, J. J.; Dooley, K. M.; Serrano, D. P.; Sousa-Aguiar, E. F.; Tada, M.; Kuhn, J.; Jaras, S. G.; Parvulescu, V.; Matsushima, T.; Murzin, D.; de Klerk, A. *Catalysis*; The Royal Society of Chemistry: London, UK, 2011; Vol. 23, pp 349−360.
(21) Chiang, H.; Bhan, A. *J. Catal.* **2010**, *271*, 251−261.
(22) Kalló, D.; Knözinger, H. *Chem. Ing. Technol.* **1967**, *39*, 676−680.
(23) Jenness, G. R.; Christiansen, M. A.; Caratzoulas, S.; Vlachos, D. G.; Gorte, R. J. *J. Phys. Chem. C* **2014**, *118*, 12899−12907.
(24) Chokkaram, S.; Srinivasan, R.; Milburn, D. R.; Davis, B. H. *J. Mol. Catal. A: Chem.* **1997**, *121*, 157−169.
(25) Kieffer, R.; Hinderman, J. P.; El Bacha, R.; Kiennemann, A.; Deluzarche, A. *React. Kinet. Catal. Lett.* **1982**, *21*, 17−21.
(26) Joubert, J.; Delbecq, F.; Sautet, P. *J. Catal.* **2007**, *251*, 507−513.
(27) Skinner, M. J.; Michor, E. L.; Fan, W.; Tsapatsis, M.; Bhan, A.; Schmidt, L. D. *ChemSusChem* **2011**, *4*, 1151−1156.
(28) Chavez Diaz, C. D.; Locatelli, S.; Gonzo, E. E. *Zeolites* **1992**, *12*, 851−857.
(29) Christiansen, M. A.; Mpourmpakis, G.; Vlachos, D. G. *ACS Catal.* **2013**, *3*, 1965−1975.
(30) Knözinger, H.; Scheglila, A.; Watson, A. M. *J. Phys. Chem.* **1968**, *72*, 2770−2774.
(31) Knözinger, H.; Scheglila, A. *J. Catal.* **1970**, *17*, 252−263.
(32) Shimizu, K.; Kon, K.; Shimura, K.; Hakim, S. S. M. A. *J. Catal.* **2013**, *300*, 242.
(33) Nondek, L.; Sedláček, J. *J. Catal.* **1975**, *40*, 34.
(34) Li, M.; Wu, Z.; Overbury, S. H. *J. Catal.* **2013**, *306*, 164.
(35) Phung, T. K.; Lagazzo, A.; Rivero Crespo, M. Á; Sánchez Escribano, V.; Busca, G. *J. Catal.* **2014**, *311*, 102−113.
(36) Wischert, R.; Copéret, C.; Delbecq, F.; Sautet, P. *Angew. Chem., Int. Ed.* **2011**, *50*, 3202−3205.
(37) Wischert, R.; Laurent, P.; Copéret, C.; Delbecq, F.; Sautet, P. *J. Am. Chem. Soc.* **2012**, *134*, 14430−14449.

(38) Amenomiya, Y.; Chenier, J. H. B.; Cvetanovic, R. J. *J. Catal.* **1967**, *9*, 28−37.
(39) Digne, M.; Sautet, P.; Raybaud, P.; Euzen, P.; Toulhoat, H. *J. Catal.* **2002**, *211*, 1−5.
(40) Parry, E. P. *J. Catal.* **1963**, *2*, 371−379.
(41) Morterra, C.; Magnacca, G. *Catal. Today* **1996**, *27*, 497−532.
(42) Wischert, R.; Florian, P.; Copéret, C.; Massiot, D.; Sautet, P. *J. Phys. Chem. C* **2014**, *118*, 15292−15299.